

TRANSMISSION X-RAY DIFFRACTION OF UNDISTURBED SOIL MICROFABRICS OBTAINED BY MICRODRILLING IN THIN SECTIONS

L. DENAIX,¹ F. VAN OORT,² M. PERNES,² AND A.G. JONGMANS³

¹ Unité d'Agronomie INRA, Domaine de la Grande Ferrade, BP 81, 33883 Villenave d'Ornon Cedex, France

² Unité de Science du Sol, INRA, Route de St.-Cyr, 78026 Versailles Cedex, France

³ Department of Soil Science and Geology, Agricultural University, P.O. Box 37, 6700 AA Wageningen, The Netherlands

Abstract—Clay mineralogical studies by X-ray diffraction performed on extracted <2- μm fractions do not always represent all clay mineral constituents present in the soil. In this work, transmission X-ray diffraction (TXRD) was applied to undisturbed microsamples of optically homogeneous mineral soil fabrics and features. These microsamples were isolated by microdrilling their periphery in soil thin sections, then removing them, and transferring them to glass capillaries for TXRD analysis. The usefulness of this technique for supplying *in situ* mineralogical information on identification, structure, and natural orientation of soil constituents was tested on mineral microfabrics and features of primary and secondary phyllosilicates. The study demonstrated that TXRD allowed detailed, representative interpretations of undisturbed mineral features and fabrics. In particular, this technique allowed us (1) to compare mineralogical compositions at selected microlocalities, (2) to study natural preferred orientations, and (3) to detect small amounts of minor mineral interstratification phases. In addition, complementary information on crystallography and crystal chemistry may be obtained by performing analytical transmission electron microscopy on the same microsample.

Key Words—Clay Fabrics, Clay Minerals, Microdrilling, Micromorphology, Transmission X-ray Diffraction, Undisturbed Microsamples.

INTRODUCTION

X-ray diffraction (XRD) is widely used to identify minerals in the clay fractions (<2 μm) extracted from bulk soil samples. To obtain purified mineral fractions, either the optimization of physical and chemical dispersion of bulk soil samples or the use of special techniques to extract microquantities of homogeneous soil constituents are required. Chemical as well as physical dispersion techniques generally are unsatisfactory for obtaining distinct and well-purified mineral phases (Tamura, 1957; Mehra and Jackson, 1965; Churchman and Weissmann, 1995; Ducaroir and Lamy, 1995; van Oort *et al.*, 1995). New approaches based on the study of microquantities of pure mineral phases have been developed. They allow the analyst to combine the location of constituents in the soil matrix by light microscopy with the analysis of their nature, crystallography, and chemical composition by XRD and analytical electron microscopy (AEM).

One approach is based on the use of microquantities ($\ll 1$ mg) of clay powder obtained by microdrilling in thin sections (Verschure, 1978; Beaufort *et al.*, 1983). XRD analyses of such small quantities require modifications of the diffraction equipment mounting. For instance, Meunier and Velde (1982) used step-scan XRD with a proportional detector to identify minerals in very small quantities of clay (10^{-1} – 10^{-2} mg). To produce clay-powder samples, they recommended the use of rod-source ultrasonics applied directly to thin sections. Rassineux *et al.* (1988) improved the quality of diffractograms of 10^{-3} -mg powder clay samples and

reduced data acquisition time by using a linear localization detector. Although study of disturbed subsamples extracted from thin sections provides useful information on the nature of mineral constituents, the procedure precludes the investigation of their fabric and natural orientation.

Another approach is to separate undisturbed microsamples from thin sections (van Oort *et al.*, 1994), so that micromorphology and analytical transmission electron microscopy (ATEM) can be performed on the same undisturbed microsample that is <50 μm in diameter. The major advantage of this technique is the ability to scale data from nanometer size to higher levels of soil structure (Jongmans, 1994). However, in ATEM studies, chemical and mineralogical data are generally restricted to small numbers of particles which are not always representative of the crystallite population. Therefore, we introduce transmission X-ray diffraction (TXRD) as a new application to the study of undisturbed soil microfeatures obtained by microsampling thin sections. Use of a transmission mounting on such microsamples allows us not only to minimize convolution effects due to sample thickness (Drits and Tchoubar, 1990) but also to examine the preferred orientation of crystallites at a submillimeter scale. Indeed, orientation of particles enhances specific (*hkl*) reflections (Wiewiora, 1982).

The present work illustrates that TXRD can give complementary *in situ* mineralogical information on the nature, structure, and natural orientations of soil mineral constituents in isolated microfabrics and al-

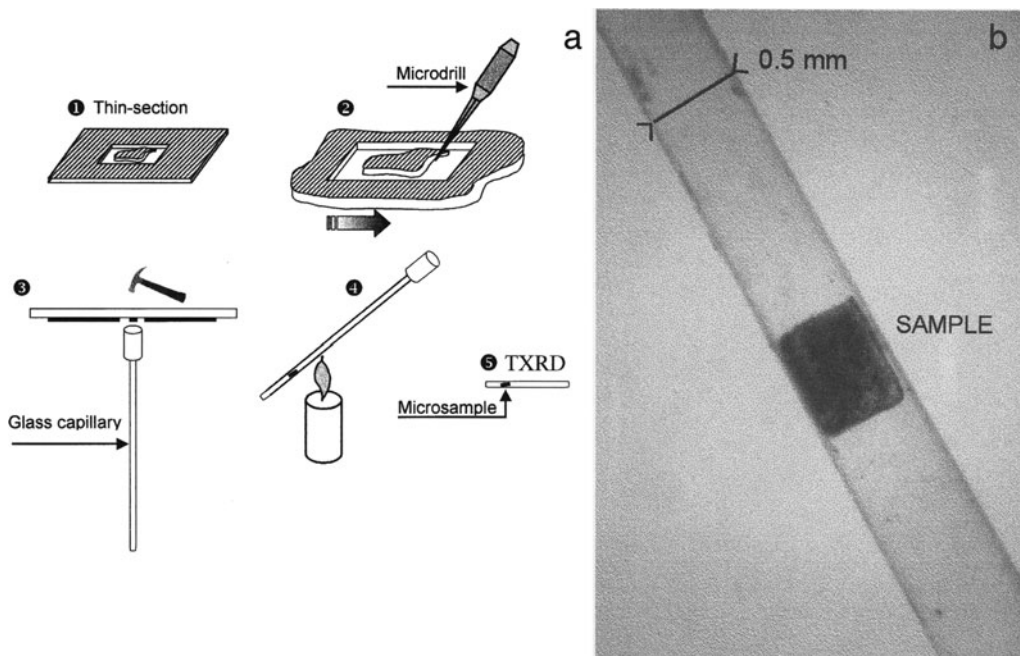


Figure 1. (a) Schematic presentation of the technical procedure for separating undisturbed microparts of thin section using microdrilling. 1) isolation of a selected mineral microfeature by removal of surrounding soil material using microdrilling; 2) loosening of the microfeature by moving the micro-stage and the micro-drill in opposite directions; 3) transferring into a Lindemann capillary; 4) sealing of the glass capillary before introduction in the TXRD mounting; 5) the finished capillary with microsample. (b) Disposition inside a Lindemann glass capillary of an undisturbed microsample from thin section.

tered phenocrysts. Therefore, we first compare a TXRD pattern obtained on an undisturbed microsample of the groundmass separated from a thin section with a diffraction pattern obtained on a randomly oriented powder <2- μm fraction extracted from the same soil. Secondly, TXRD is demonstrated on microfeatures of primary and secondary phyllosilicates separated from thin sections from tropical and temperate volcanic soils to determine the textural properties of clay minerals and to assess the presence of small amounts of minor but distinct clay phases.

MATERIALS AND METHODS

Techniques

Uncovered thin-sections were prepared according to the procedure of FitzPatrick (1970) and Miedema *et al.* (1974) using a polyester resin. Micromorphological interpretation uses the terminology of Bullock *et al.* (1985). Mineral fabrics and features were selected under a petrographic microscope. The uncovered thin section was placed in a microscope-stage-mounted micromanipulator to give a controlled horizontal sample movement. Microsampling of undisturbed features was performed with a microscope-mounted drill (Verschure, 1978) which can be moved in a vertical direction, and which has a hardened stainless steel needle point, sharpened to a 20- μm tip. Isolation of a microsample started with removal of all surrounding soil

material by microdrilling (Figure 1a, step 1) so that the cleaned microsample is only connected to the underlying glass slide. The tip of the nonrotating drill was placed against the microsample, and the latter loosened by moving it carefully against the tip of the drill (step 2). A Lindemann glass capillary was placed on the microsample and the thin section was turned upside down (step 3). The sample was thus transferred to the bottom of the glass capillary which was subsequently sealed by heating (step 4). To avoid displacement of the sample in the capillary the capillary size (0.3 or 0.5 mm) was adapted to the sample size (Figure 1b).

TXRD studies were performed using a Siemens D5000 diffractometer in transmission geometry with a focusing Ge primary monochromator using $\text{CuK}\alpha$ radiation (40 kV, 30 mA), a linear position-sensitive detector (Elphyse), and a rotatable capillary sample holder (Figure 2). This device is adjustable in translation and rotation to center the sample and to allow selection of preferred angles (ϕ) of the sample surface with respect to the X-ray beam. Soller slits and a primary variable slit (~ 1 mm) were placed in front of the sample. The selected beam size was 0.2×5 mm for all experiments. The diffractometer was calibrated using quartz as an external standard. Experiments were made either with a selected constant angle (ϕ) between the surface of the microsample and the incident X-ray

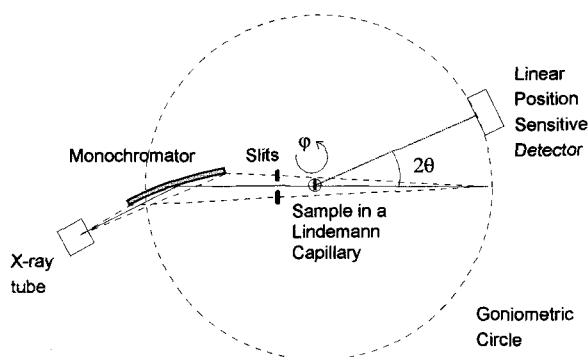


Figure 2. Schematic view of the TXRD mounting.

beam or using the rotation mode. The latter procedure allowed integration of all the XRD reflections of the crystallites and was comparable to a classical randomly oriented powder diffractogram. Counting time was 500 $s/2\theta$; the step size was 0.016 $^{\circ}2\theta$. A randomly oriented powder diffractogram on extracted fractions of $<2 \mu\text{m}$ was obtained under the same conditions. The data were analyzed with Diffrac-AT software (SOCABIM), the continuous background was subtracted, if necessary, and the resulting diffractograms were compared with JCPDS files.

Soil samples

To illustrate both the usefulness and the limits of this technique, several samples with distinct characteristics were studied. Mineral features were extracted from thin sections selected from B and C horizons of four soils with an important volcanic rock component. Information for these sampled horizons is summarized in Table 1. Two soils of the temperate regions were sampled in the Massif Central (France). At the Buhlon site, at 120 cm depth, a clayey, illuvial B horizon (Btg_2) of a paleosol developed on a Pleistocene Allier terrace is composed of soft, white, rounded trachytic pumice fragments as well as fresh and partially weathered volcanic and granite fragments (Feijtel *et al.*, 1989; Jongmans *et al.*, 1991). Microsamples of primary phyllosilicates (micas) were studied. At the Puy-de-Mur site, weathering of Miocene-Pliocene basaltic volcanic deposits led to formation of smectitic, clay-rich soils. Here, microfeatures of clay pseudomorphs after olivine were studied. On the volcanic island of Basse Terre (Guadeloupe, French West Indies), highly weathered porphyric andesitic saprolites that formed

under tropical perudic climatic conditions were sampled. Ferrallitic weathering led to isovolumetric transformation of all weatherable primary minerals into secondary soil constituents and, consequently, significant leaching of silica and basic cations. Feldspars transformed either to halloysitic clay or gibbsite pseudomorphs. Pyroxenes transformed dominantly into open clay-iron boxwork pseudomorphs (Delvigne, 1983) partly composed of phyllosilicates with 2:1 layers (van Oort *et al.*, 1995) as a result of hypogene (Delvigne, 1990), an early-stage hydrothermal, alteration. Two samples were chosen, located in two distinct soils (Table 1). At the Solitude site, clay infillings in former intramineral cracks of a pyroxene were studied. At the Morne-à-Louis site, the groundmass of the saprolite was sampled in thin section.

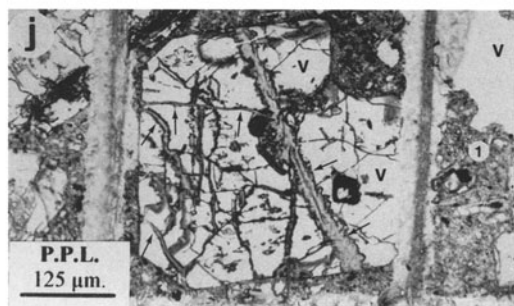
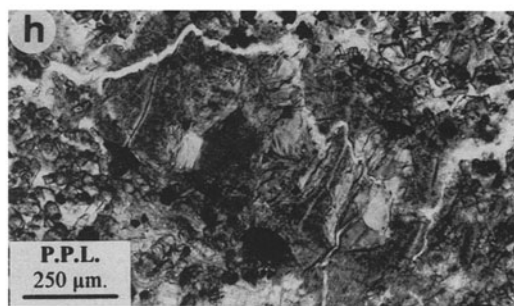
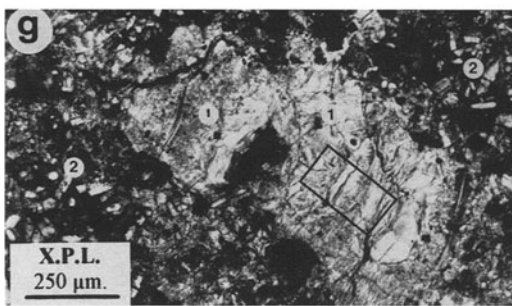
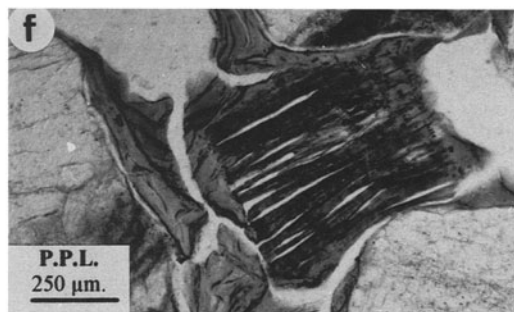
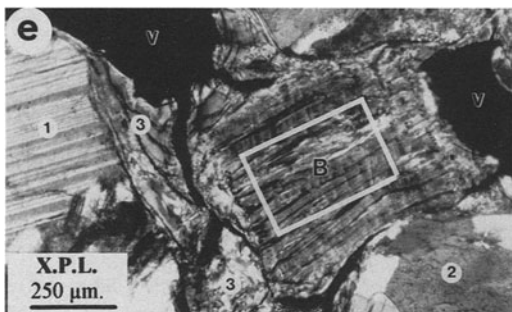
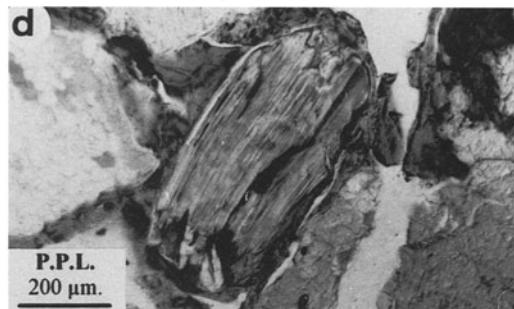
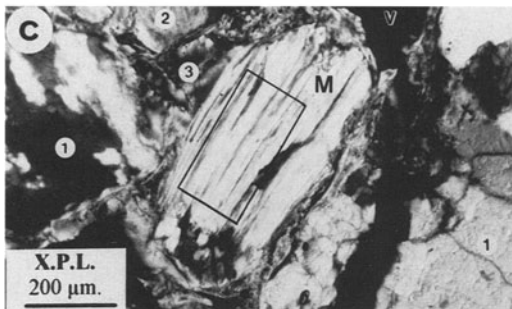
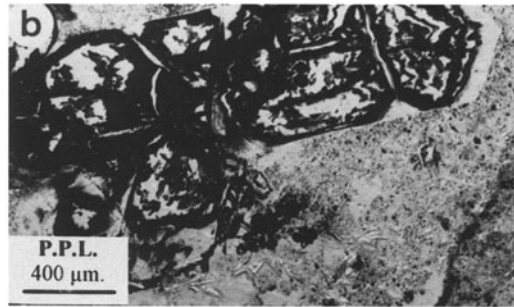
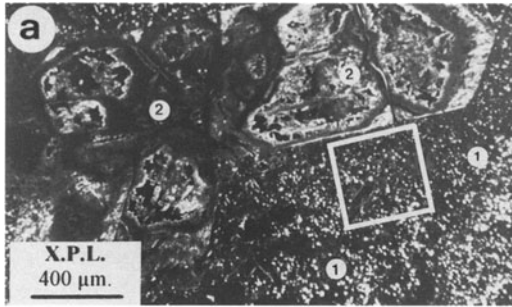
RESULTS

Features of the groundmass

Morne-à-Louis site. Thin sections (Figure 3) of the andesitic saprolite show clay pseudomorphs after primary minerals such as feldspar and pyroxene as large as a few mm (Figure 3a). In the fine-textured isotropic to weakly anisotropic groundmass, white strongly anisotropic crystals to $5 \mu\text{m}$ were observed in polarized light and optically identified as gibbsite (Figure 3a). Well-crystallized magnetite and poorly crystalline iron oxide compounds occur as well (Figure 3b). An undisturbed microsample of $0.5 \times 0.5 \times 0.03 \text{ mm}$. ($\sim 7.5 \mu\text{g}$) was separated from the groundmass of the saprolite (Figure 3a). The background-corrected TXRD pattern showed a large number of well-defined diffraction peaks (Figure 4a). The spectrum was obtained in rotation mode to avoid preferential orientation and to compare it with a diffraction pattern of a randomly oriented clay-powder sample. Eight mineral phases were identified. Twenty-five hkl reflections of gibbsite (JCPDS 7-0324) were observed, with relative intensities I/I_0 as low as 1%. The most important peaks for magnetite ($d = 0.297, 0.253, 0.162 \text{ nm}$), cristobalite ($d = 0.405 \text{ nm}$), tridymite ($d = 0.409, 0.382 \text{ nm}$), and anatase ($d = 0.352, 0.189, 0.169, 0.166 \text{ nm}$) were identified. A small but significant peak ($d = 0.417 \text{ nm}$) was also detected and attributed to goethite. An asymmetric basal (001) reflection centered at 0.718 nm, a broad (002) reflection centered at 0.356 nm, and two diffraction peaks at 0.1485 and 0.1480 nm, attributed to (060) reflections, indicate the presence of diocta-

Table 1. General characteristics of studied samples. Terminology according to guidelines of Soil Survey Staff (1998).

Sample site	Location	Temperature regime	Moisture regime	Soil type	Horizon	Depth (cm)
Buhlon	Massif Central	Mesic	Udic	Typic Albaquult	Btg_2	120
Puy-de-Mur	Massif Central	Mesic	Udic	Typic Eutrodept	R/C	>180
Solitude	Guadeloupe	Isohyperthermic	Perudic	Typic Haploperox	R/C	150
Morne-à-Louis	Guadeloupe	Isohyperthermic	Perudic	Typic Haploperox	C	>100



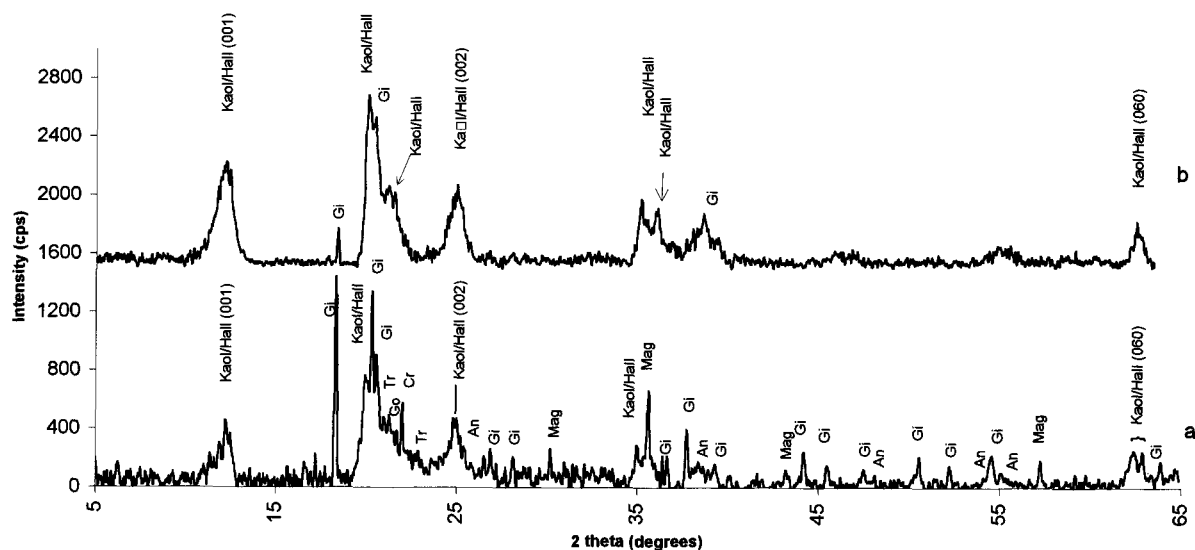


Figure 4. TXRD pattern in scanning mode from Morne-à-Louis samples, 5–65 $^{\circ}2\theta$ range, (a) microsample of groundmass ($\sim 7.5 \mu\text{g}$) and (b) $<2\text{-}\mu\text{m}$ powder sample of clay fraction extracted from bulk soil sample ($\sim 2 \text{mg}$). An: Anatase, Cr: Cristobalite, Gi: Gibbsite, Go: Goethite, Hall: Halloysite, Kaol: Kaolinite, Mag: Magnetite, Tr: Tridymite.

hedral 1:1 phyllosilicates. Figure 4b is the XRD pattern obtained on a powder sample ($\sim 2 \text{mg}$) of the $<2\text{-}\mu\text{m}$ fraction. Only two mineral phases were identified in this pattern by characteristic but rather broad diffraction peaks attributed to a dioctahedral 1:1 phyllosilicate and to gibbsite.

Features in primary phyllosilicate minerals

Bulhon site. In this sample, single mica grains, from disintegrated granite fragments were observed. Muscovite (Figure 3c and 3d) and biotite (Figure 3e and 3f) displayed pellicular and parallel banded alteration due to ongoing weathering. Biotite was partially stained along the cleavage planes and occasionally the grains showed argillization. In addition, outer margins of some muscovite grains displayed a shift from the original interference colors to pale yellow, suggesting an initial argillization of this mineral as well. Both minerals were usually embedded in nonlaminated, isotropic to weakly anisotropic, limpid coatings and infillings of allophane (Jongmans *et al.*, 1994) and/or randomly oriented halloysite (van Oort *et al.*, 1994). TXRD diagrams of an undisturbed muscovite microsample ($\sim 3 \mu\text{g}$) are shown in Figure 5a and 5b. The

overall TXRD spectrum (not shown) revealed all characteristic diffraction peaks of a muscovite- $2M_1$ (JCPDS 6-0263). In the range 4–16 $^{\circ}2\theta$, ~ 20 experiments with the angle (ϕ) varying between the surface of the microsample and the X-ray beam were performed with steps of $10^{\circ} \phi$ from a parallel position ($0^{\circ} \phi$) to a perpendicular position ($90^{\circ} \phi$) and on to the opposite parallel ($180^{\circ} \phi$) position. A $d(001)$ basal reflection at 1.0 nm was observed between $60\text{--}150^{\circ} \phi$. Within a very narrow angle range, the $d(001)$ reflection reached its maximum and sharpest intensity. The presentation of $d(001)$ intensity as a function of ϕ angle (Figure 5c) and simulated by two Gaussian distributions suggested the presence of two crystallite populations. The first phase is a very well-oriented, 1.0-nm muscovite with the maximum reflection in the $80^{\circ} \phi$ position. This position is considered as the reference position. A second 1.0-nm phase, apparently less well oriented or more finely divided, produced an additional $d(001)$ reflection in the ϕ range $60\text{--}150^{\circ}$. This second population is a mica-illite interstratification. This latter phase was observed optically to have lower interference colors present in the muscovite grains as is common in mica-illite. The presence of illite in deeper

←

Figure 3. Micromorphological images of microfibrils isolated by microdrilling in thin sections. XPL = crossed-polarized light, PPL = plane-polarized light, v = void, [] = selected microparts. (a) and (b) fine grained soil groundmass (1) and clay and iron pseudomorph after pyroxene (2) (Morne-à-Louis, saprolite); (c) and (d) muscovite (M), with quartz (1), volcanic rock fragments (2), and strong anisotropic clay coatings (3) (Bulhon, Btg₂ horizon); (e) and (f) biotite (B), with feldspar (1), quartz (2), and strong anisotropic clay coatings (3) (Bulhon, Btg₂ horizon); (g) and (h) total clay pseudomorph after olivine (1) in unweathered volcanic rock (2) with feldspars, magnetite, and volcanic glass (Puy-de-Mur, R/C horizon); (i) and (j) iron-oxide coated clay infillings (→) in an open clay-iron boxwork pseudomorph after pyroxene, within a pedoplasmated soil groundmass (1) (Solitude, C horizon).

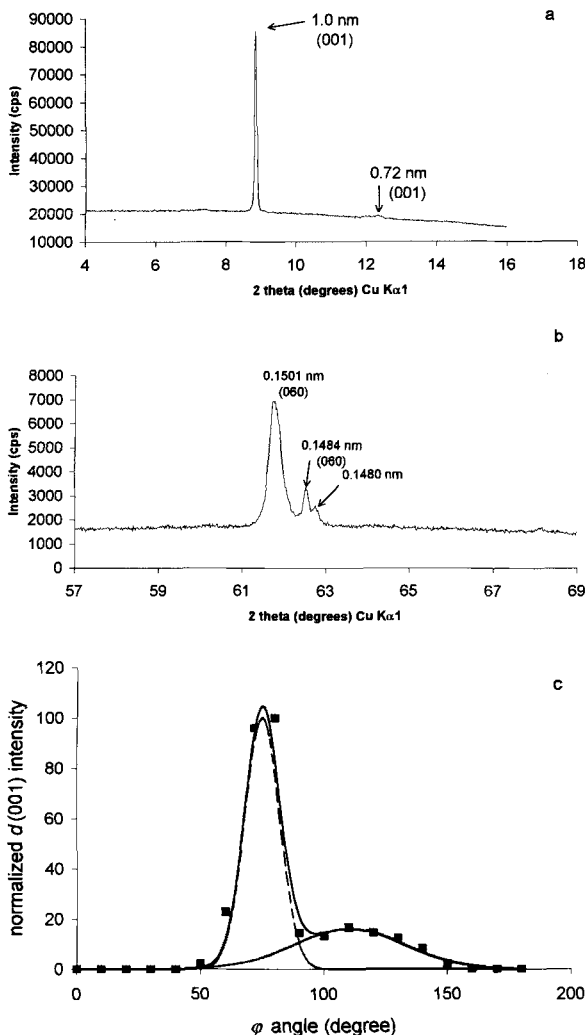


Figure 5. TXRD of a muscovite microsample from Buhlon, (a) 4–16 $^{\circ}2\theta$ range, 80° - ϕ position and (b) 57–69 $^{\circ}2\theta$ range, 170° - ϕ position; (c) Muscovite microsample from Buhlon. Normalized diffracted intensity (Intensity at a given ϕ position/Maximum experimental diffracted intensity \times 100) of the 1.0-nm peak as a function of ϕ position. Experimental data (■); simulated curve (—) summing the simulated curves of two crystallite populations; a well-oriented phyllosilicate population (---); and a less well-oriented phyllosilicate population (- - -).

horizons of older Allier terraces in which this profile developed was previously reported by Jongmans *et al.* (1991). Another basal reflection, centered at 0.72 nm, was observed for the 80° - ϕ reference position (Figure 5a), but it disappeared with an increase in inclination to 90° ϕ . This reflection indicates a small amount of possibly very fine grained 1:1 phyllosilicates. For the 80° - ϕ reference position, TXRD analysis performed in the perpendicular position, 170° ϕ , showed characteristic *hk* reflections. The resulting pattern, showing a very strong *d*(060) reflection of dioctahedral mica (*d* = 0.1501 nm), was observed as well as two additional

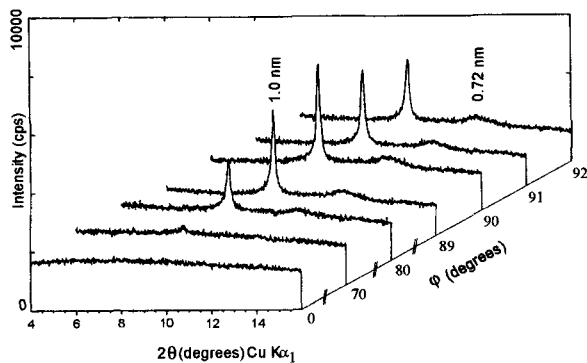


Figure 6. Three-dimensional TXRD pattern of biotite microsample from Buhlon, ϕ angle on z axis.

peaks, at 0.1484 and 0.1480 nm (Figure 5b). The 0.1484-nm peak is the *d*(060) reflection of a dioctahedral phyllosilicate comprising 1:1 layers, the latter is an *hk* reflection of dioctahedral mica. In the reference position, no *d*(060) reflections can be detected, underlining the strong natural orientation of both muscovite and the 1:1 phyllosilicates.

Similar diffractograms were obtained for a microsample of biotite ($\sim 6 \mu\text{g}$). The optimum orientation for the biotite (001) peak (Figure 6) lay between ~ 70 – 110° ϕ . Maximum intensity of (001) was observed for 90° ϕ ; an inclination of only 1° ϕ caused a notable decrease of intensity. As before, a secondary mineral comprising 1:1 layers occurs in parallel orientation with the biotite. This is consistent with the optical observations of the mineral in the initial stages of argillization.

Features of secondary phyllosilicate minerals

Puy-de-Mur site. The weathering zone of basaltic volcanic deposits from the Puy-de-Mur site contain many strong anisotropic, euhedral clay-pseudomorphs after 0.5 to 2 mm diameter olivine. The yellowish to yellowish-green clay displays a stipple-speckled *b*-fabric and a mosaic of strongly oriented flakes with continuous birefringence (Figure 3g and 3h). These clay fabrics are embedded in a fine-grained, weakly altered groundmass, consisting dominantly of feldspars and magnetite. A microsample of $<1 \mu\text{g}$ was separated from a clay pseudomorph after olivine and studied by TXRD. In the low-angle range (Figure 7a), a broad but distinct peak was centered at 1.45 nm, corresponding to the (001) reflection of a phyllosilicate with 2:1 layers. A second, very broad and very weakly developed band occurs at 1.03 nm. Under moderate leaching conditions, weathering of olivine and pyroxene in basaltic rocks frequently leads to formation of chloritic and/or smectitic clay minerals (Huang, 1989; Jongmans *et al.*, 1994). Several factors may explain the breadth and the poor definition of the (001) diffraction bands observed in Figure 7a: 1) the presence of fine-

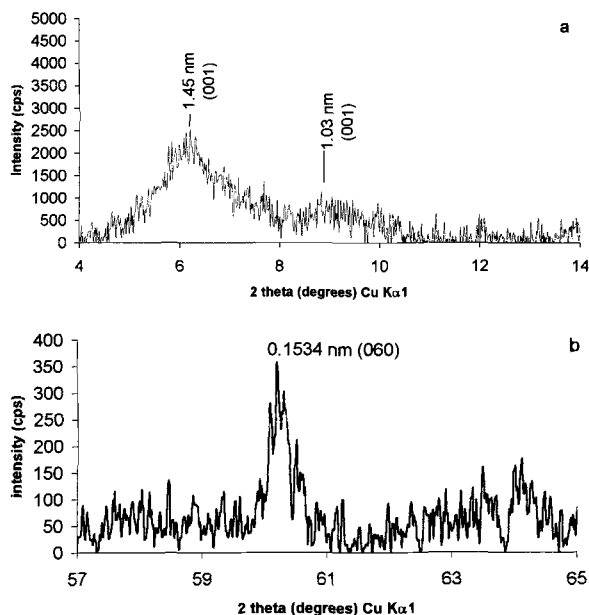


Figure 7. TXRD pattern of microfabric of clay pseudomorph after olivine from Puy-de-Mur, (a) 4–14 °2θ range, and (b) 57–65 °2θ range.

grained, poorly crystalline chlorite, 2) at the nanometer scale, pedogenetic smectite formed in clay pseudomorphs generally shows disordered layer stacking (van Oort *et al.*, 1995), 3) sample inclusion by polyester resin may disturb the natural arrangement of clay quasicrystals and domains, and 4) during impregnation of *in situ* clay fabrics, the cation composition of interlayer spaces is not controlled. In the 57–65 °2θ range (Figure 7b), a distinct (060) reflection observed at 0.1534 nm suggests a trioctahedral 2:1 phyllosilicate (Moore and Reynolds, 1989).

TXRD at different ϕ angles shows no preferred orientation of clay minerals in this microsample. Micromorphology showed strong anisotropic clay domains (20–50 μm in diameter) with a mosaic distribution pattern within the clay-pseudomorph. This distribution explains the absence of preferred orientation in the TXRD patterns. The sample is composed of an aggregate of well-oriented individual domains in a random distribution.

Solitude site. In the weathering rinds adjacent to fresh rock cores, pyroxene phenocrysts (often >200 μm) display cross-banded alteration patterns. Strongly denticulated pyroxene residue surfaces and the surrounding voids are bordered by limpid clay frameworks, which are pre-existing intramineral clay-infillings in the original pyroxene mineral (van Oort *et al.*, 1995) produced by hypogene weathering. With increasing distance from the unaltered andesitic rock, pyroxene residues completely disappear, and the clay framework progressively becomes impregnated and covered by

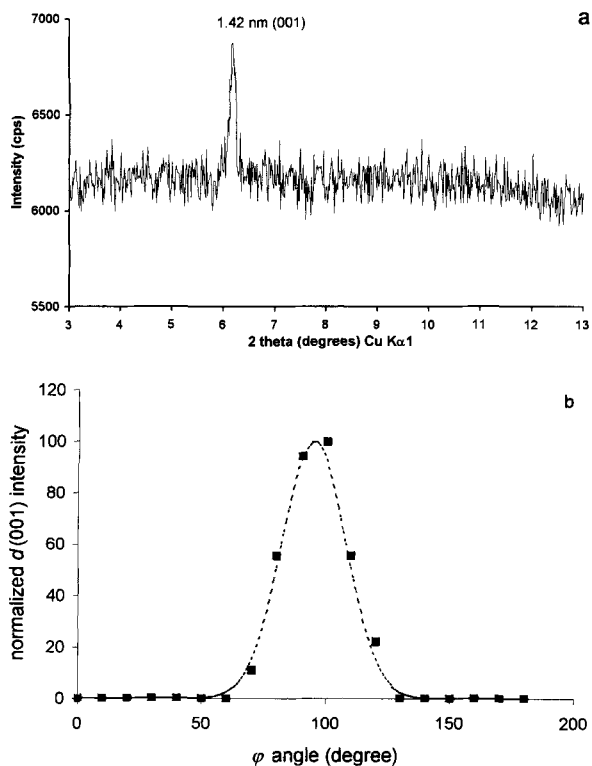


Figure 8. (a) TXRD pattern of microfabric of clay infilling from Solitude, 3–13 °2θ range, 90° ϕ position and (b) Microfabric of clay infilling from Solitude. Normalized diffracted intensity (Intensity at a given ϕ position/Maximum experimental diffracted intensity $\times 100$) of the 1.42-nm peak as a function of ϕ position. Experimental data (■); simulated curve (---).

20–50- μm thick Fe oxide coatings. The initial pyroxene phenocryst was transformed into an open compound boxwork pseudomorph, consisting dominantly of poorly crystalline iron and clay (Figure 3i and 3j). A microsample of the clay-infilling of $\sim 0.5 \mu\text{g}$ was selected for TXRD.

In the range from 3 to 13 °2θ, TXRD was performed by varying the angle (ϕ) between the surface of the microsample and the X-ray beam to investigate the possible natural orientation. A distinct 1.42-nm X-ray diffraction band appeared between $\phi = 80$ – 110° , with the maximum intensity between $\phi = 90$ – 100° (Figure 8a and 8b). A strong decrease ($\sim 25\%$) was observed when ϕ was changed by $\pm 10^\circ$ from these maximum intensity peaks. The peak completely disappeared for a variation of $\pm 30^\circ$. These data indicate strong and uniform orientations of the clay particles and corroborate the micromorphological observations made with a light microscope. This diffraction band at 1.42 nm is the (001) reflection of 2:1 phyllosilicates. The presence of greenish smectitic clay minerals occurring in intramineral cracks in the fresh andesitic rocks under-

lying the soils at the Solitude site was demonstrated previously (van Oort *et al.*, 1995).

DISCUSSION

TXRD performed on undisturbed microsamples removed from soil thin sections allows detailed mineralogical study at scales compatible with light microscopy. This scale of analysis is essential in many studies on soils and saprolites. In volcanic environments in particular, secondary soil constituents (*e.g.*, clay minerals) are often non-homogeneously distributed as a result of neogenesis in specific microenvironments, impregnation and cementation processes, or pedological redistribution (Delvigne and Stoops, 1990; Nahon, 1990; van Oort *et al.*, 1990, 1995; Jongmans, 1994). Hence, the major interest of the new technique lies in obtaining precise mineralogical information on optically homogeneous clay features from distinct locations in the soil profile.

For example, the TXRD pattern of the groundmass of Morne-à-Louis (Figure 4a) shows that at least five mineral phases (gibbsite, magnetite, tridymite, anatase, and 1:1 phyllosilicates) can be unambiguously identified and the presence of two more minerals (cristobalite and goethite) is suggested. Secondary mineral constituents occurring in specific micro-localities may represent small quantities with respect to the bulk clay fraction. Consequently these phases can be easily overlooked in routine XRD analyses of the <2- μm clay fraction. The comparison of the two spectra of the undisturbed microsample (Figure 4a) and the sample containing the <2- μm fraction (Figure 4b) of the groundmass of Morne-à-Louis, clearly demonstrates the inappropriateness of the common assumption that groundmass consists only of the <2- μm fraction. In fact, the interpretation of a powder diffractogram of the extracted <2- μm size fraction depends on the (arbitrary) size of the minerals. Non-randomly distributed mineral phases in the groundmass (for example, secondary cristobalite, magnetite in the Morne-à-Louis microsample, Figure 4) are either not included in the extracted clay sample or overlooked because they are diluted by the dominant clay constituents. Moreover, extraction of the <2- μm size fraction minimizes heavy, fine-grained particles. An additional difficulty with clay samples is the problem of preparing a sample containing a truly randomly oriented powder for XRD analysis. In Figure 4b, 00 l reflections of layer silicates apparently were optimized in comparison to the hk reflections, suggesting a partial orientation of the powder during XRD sample preparation.

The proposed technique is useful not only for local mineralogical identification but also for mineral-orientation studies. Indeed, preservation of the natural orientation of soil clay microfibrils in the TXRD sample allows the textures and crystallographic orienta-

tions to be studied. The power of a combination of TXRD and ATEM for such studies is obvious.

However, the strength of this technique defines its limitations as well. The presence of "foreign matter" between the silicate layers (*e.g.*, organic materials, iron and/or aluminium oxy-hydroxides, amorphous silica) may lead to irregular layer stacking (Brindley, 1980; Whittig and Allardice, 1986) and therefore restrict the study, for example, to 00 l reflections. The use of polyester resin impregnated microsamples from thin sections limits the destruction of specific phases (*e.g.*, organic matter, Fe oxide coatings) although removal of iron oxide was reported by Bullock *et al.* (1975). For the same reasons, reorientation of clay minerals in microsamples to enhance the (00 l) reflections is precluded. Chemical tests, currently used for improving identification of phyllosilicates can not be applied, *e.g.*, uniform cation saturation, glycerol solvation to identify swelling clay minerals, formamide to distinguish halloysite and kaolinite, heating, *etc.*

Applying TXRD on microsamples is a time-consuming technique and is not meant to be used in routine analyses. Working with very small amounts of material results in increased counting times of several days for each ϕ position. For the 0.5- μg microsample of the Solitude clay infilling, the TXRD patterns remained noisy, despite these long counting times (Figure 8a). This example illustrates another limit of the technique.

Finally, note that this technique has the potential to provide valuable data of a representative population of mineral particles at the micrometer scale. Such data allows valid upscaling from the nanometer and micrometer scale to higher levels of soil organization. A micromorphological study is a convenient method for estimating the importance of a given type of microfabric or microfeature. The combination of light microscopy and TXRD on undisturbed microsamples separated from soil thin sections allows detailed and localized mineralogical studies of heterogeneous samples.

CONCLUSION

A new technique of TXRD has been developed that can be used to analyze microsamples of soils ranging from 10 to 0.5 μg with preserved *in situ* arrangements of particles and features. This technique allows direct study of secondary mineralogical transformations within single primary mineral grains. Compared to classical mineralogy studies on <2- μm separates, the technique minimizes artifacts that may be generated by chemical sample treatments (dispersion, selective dissolution) which are conventionally applied during XRD clay-sample preparation procedures. The combination of optical microscopy and TXRD improves mineralogical identification as well as the study of the structure and natural orientation of neofomed clay

minerals and fabrics. Furthermore, TXRD studies can be performed along crystal-growth axes which reflect structures of former primary minerals, or directions of intramineral cracks. Knowledge of the crystallographic orientations, for example, permits proper orientation for re-embedding the sample for ultramicrotomy and a subsequent ATEM study. A complete mineralogical approach, relating mineralogical aspects (TXRD) and crystal chemical composition (ATEM) of soil constituents to their location in the soil (optical microscopy) may produce a better understanding of weathering processes and soil behavior.

ACKNOWLEDGMENTS

The authors thank M.L. Thompson for his critical reading and valuable suggestions and D. Beaufort for his constructive comments.

REFERENCES

- Beaufort, D., Dudoignon, P., Proust, D., Parneix, J.C., and Meunier, A. (1983) Microdrilling in thin sections: A useful method for the identification of clay minerals in situ. *Clay Minerals*, **18**, 223–226.
- Brindley, G.W. (1980) Order-disorder in clay mineral structures. In *Crystal Structures of Clay Minerals and Their X-ray Identification*. G.W. Brindley and G. Brown, eds., Mineralogical Society, Monograph No. 5, London, 125–195.
- Bullock, P., Loveland, P., and Murphy C.P. (1975) A technique for selective solution of iron oxides in thin sections of soil. *Journal of Soil Science*, **26**, 247–249.
- Bullock, P.N., Fédoroff, N., Jongerius, A., Stoops, G., and Tursina, T. (1985) *Handbook for Soil Thin Section Description*. Waine Research Publications, Albrighton, England, 150 pp.
- Churchman, G.J. and Weissmann, D.A. (1995) Separation of sub-micron particles from soils and sediments without mechanical disturbance. *Clays and Clay Minerals*, **43**, 85–91.
- Delvigne, J. (1983) Micromorphology of the alteration and weathering of pyroxene in the Koua Bocca ultramafic intrusion, Ivory Coast, West Africa. *Sciences Géologiques Mémoire*, **72**, 57–68.
- Delvigne, J. (1990) Hypogene and supergene alterations of orthopyroxene in the Koua Bocca ultramafic intrusion, Ivory Coast. *Chemical Geology*, **84**, 49–53.
- Delvigne, J. and Stoops, G. (1990) Morphology of mineral weathering and neoformation: I Weathering of most common silicates. In *Soil Micromorphology: A Basic and Applied Science*, L.A. Douglas, ed., Elsevier, Amsterdam, 471–481.
- Drits, V.A. and Tchoubar, C. (1990) *X-ray Diffraction by Disordered Lamellar Structures. Theory and Applications to Microdivided Silicates and Carbons*. Springer-Verlag, Heidelberg. 371 pp.
- Ducaroir, J. and Lamy, I. (1995) Evidencing of trace metal association with soil organic matter using particle size fractionation after physical dispersion treatment. *Analyst*, **120**, 741–745.
- Feijtel, T.C.J., Jongmans, A.G., and van Doesburg, J.D.J. (1989) Identification of clay coatings in an older Quaternary terrace of the Allier, Limagne, France. *Soil Science Society of America Journal*, **53**, 876–882.
- Fitzpatrick, E.A. (1970) A technique for the preparation of large thin sections of soils and consolidated material. In *Micromorphological Techniques and Application*, D.A. Osmond and P. Bullock, eds., Technical Monograph 2, Soil Survey of England and Wales, Rothamsted, Harpenden, 3–13.
- Huang, P.M. (1989) Feldspars, Olivines, Pyroxenes, and Amphiboles. In *Minerals in Soil Environments*, J.B. Dixon and S.B. Weed, eds., Soil Science Society of America, Madison, Wisconsin, 975–1050.
- Jongmans, A.G. (1994) Aspects of mineral transformation during weathering of volcanic materials: The microscopic and submicroscopic level. Thesis, Wageningen University, Wageningen, The Netherlands, 143 pp.
- Jongmans, A.G., Feijtel, T.C.J., Miedema, R., van Breemen, N., and Veldkamp, A. (1991) Soil formation in a Quaternary terrace sequence of the Allier, Limagne, France. Macro- and micromorphology, particle size distribution, chemistry. *Geoderma*, **49**, 215–239.
- Jongmans, A.G., van Oort, F., Buurman, P., and Jaunet, A.M. (1994) Micromorphology and submicroscopy of isotropic and anisotropic Al/Si coatings in a quaternary Allier terrace, France. In *Soil Micromorphology, Development in Soil Science 22*, A.J. Ringrose-Voase and G.S. Humphreys, eds., Elsevier, Amsterdam, 285–291.
- Jongmans, A.G., van Oort, F., Nieuwenhuysse, A., Jaunet, A.M., and van Doesburg, J.D.J. (1994) Inheritance of 2:1 phyllosilicates in Costa Rican Andisols. *Soil Science Society of America Journal*, **58**, 494–501.
- Mehra, O.P. and Jackson, M.L. (1965) Iron oxide removal from soils and clays by a dithionite-citrate system buffered with sodium bicarbonate. *Clays and Clay Minerals*, **7**, 317–327.
- Meunier, A. and Velde, B. (1982) X-ray diffraction of oriented clays in small quantities (0.1 mg). *Clay Minerals*, **17**, 259–262.
- Miedema, R., Pape, T., and van der Waal, G.J. (1974) A method to impregnate wet soil samples, producing high-quality thin sections. *Netherlands Journal of Agricultural Science*, **22**, 37–39.
- Moore, D.M. and Reynolds, R.C. (1989) *X-ray Diffraction and Analysis of Clay Minerals*. Oxford University Press, Oxford, 322 pp.
- Nahon, D. (1990) *Introduction to the Petrology of Soils and Chemical Weathering*. John Wiley & Sons Inc, New York, 286 pp.
- Rassineux, F., Beaufort, D., Bouchet, A., Merceron, T., and Meunier, A. (1988) Use of a linear localization detector for X-ray diffraction of very small quantities of clay minerals. *Clays and Clay Minerals*, **36**, 187–189.
- Soil Survey Staff, (1998) *Keys to Soil Taxonomy, 8th edition*. United States Department of Agriculture, Natural Resources Conservation Service, 326 pp.
- Tamura, T. (1957) Identification of the 14 Å clay mineral component. *American Mineralogist*, **42**, 107–110.
- van Oort, F., Jongmans, A.G., Jaunet, A.M., van Doesburg, J.D.J., and Feijtel, T.C.J. (1990) Andesite weathering and halloysite newformation in ferrallitic soil environment in Guadeloupe. *In-situ* study of different halloysite facies on thin sections by SEM-EDXRA, microdrilling, step scan XRD and TEM. *Comptes Rendus de l'Académie des Sciences, Paris*, **310**, 425–431.
- van Oort, F., Jongmans, A.G., and Jaunet, A.M. (1994) The progression from optical light microscopy to transmission electron microscopy in the study of soils. *Clay Minerals*, **29**, 247–254.
- van Oort, F., Jongmans, A.G., and Jaunet, A.M. (1995) Optical and electron microscopy as a tool in clay mineralogy studies of accessory 2:1 phyllosilicates in volcanic soils of the humid tropics. In *Clays: Controlling the Environment, Proceedings of the 10th International Clay Conference, Adelaide (1993)*, G.J. Churchman, R.W. Fitzpatrick, and

- R.A. Eggleton, eds., CSIRO Publications, Melbourne, Australia, 449–456.
- Verschure, R.H. (1978) A microscope mounted drill to isolate microgram quantities of mineral material from polished thin sections. *Mineralogical Magazine*, **42**, 449–503.
- Wiewiora, A. (1982) Oblique texture method in transmission X-ray diffractometry of clays and clay minerals. *Proceedings 9th Clay Mineral Petrology Conference, Zvolen, 1982, Praha*, 43–51.
- Whittig L.D. and Allardice W.R. (1986) X-ray diffraction techniques. In *Methods of Soil Analysis, Part I Physical and Mineralogical Methods*, A. Klute ed., American Society of Agronomy-Soil Science Society of America, Madison, Wisconsin, 331–362.

(Received 22 May 1998; accepted 18 April 1999; Ms. 98-066)